Electronic Supplementary Material (ESI) for Journal of Materials Chemistry A

Supporting Information

Fe-N doped Carbon Nanotube/Graphene Composite: Facile Synthesis and High Electrocatalytic Activity

*Shiming Zhang, Heyou Zhang, Qing Liu and Shengli Chen**

Contents

S1. Experimental Section

S1.1 Synthesis of Graphene oxide:

Graphene oxide (GO) was prepared from graphite powder (Sigma Aldrich) by the modified Hummers method.[1] Briefly, graphite (2 g), KNO_3 (1 g) and concentrated H_2SO_4 (100 mL) were added successively to a three-neck flask equipped with mechanical stirrer. $KMnO_4$ (15 g) was gradually added to the mixture under vigorous agitation and the reaction temperature was kept below 20 °C by placing the reaction flask in an ice-water bath. The reaction system was then heated to 38 ˚C and allowed to stand for 24 h with gentle stirring, during which the mixture became more and more viscous with color gradually changing from dark green to reddish brown. After cooling with an ice bath, the reaction mixture was diluted with 300 ml deionized water, followed by addition of 10 ml of 30 wt % H_2O_2 to reduce the insoluble manganese species. In order to purify the product, the suspension was centrifuged and washed with deionized water repeatedly. The centrifugation was dialyzed until no precipitate of $BaSO_4$ was detected upon addition of a few drops of $BaCl_2$ aqueous solution. Finally, the dialysate was subject to ultrasonic exfoliation and then lyophilized to obtain fluffy GO powder.

S1.2 Synthesis of N-doped carbon materials:

To prepare the N-CNT/N-G composite, ca. 4 g melamine and different amounts of $FeSO_4 \cdot 7H_2O$ were first added into 50 mL aqueous suspension of GO of 3 mg mL^{-1} concentration, with Fe/GO mass ratios of 1:75 ~ 1:15 respectively. After thoroughly blending under ultrasonication, the mixture was dried by using a rotary evaporator at 60 ˚C. The resulted precursor mixture was then placed in a tube furnace and heated to desired temperatures (700-1000 ℃) and stayed for 1 hour under atmosphere of high purity argon, followed by naturally cooling to room temperature with continuous flowing of argon, which led to the final dark black catalyst sample. The Fe/GO ratio and the final temperature were opti-mized to obtain a most positive ORR half-wave potential ($E_{1/2}$) (Figures S5 and S6). The N-CNT and N-G were prepared by using the similar procedure but with precursor mixtures without GO and Fe salts respectively. The preparation of GO is given in the Spporting Information.

S1.3 Physical characterizations:

Scanning electron microscopy (SEM) images were obtained by HITACHI S-4800 Scanning Electron Microsope. Transmission electron microscope (TEM) images were obtained at

JEM-2100F. X-ray photoelectron spectroscopy (XPS) measurements were carried out using a Kratos Ltd. XSAM-800 spectrometer with Mg Kα radiator. The data were fitted by using Gaussian/Lorentzian fitting in the software XPSPEAK41 with Shirley function as baseline. Powder X-ray diffraction (XRD) patterns were obtained on a Shimadzu XRD-6000 X-ray diffractometer using Cu Kα radiation source operating at 40 kV and 30 mA. The XRD profiles are recorded at a scanning rate of 4°/min. The N_2 adsorption isotherms of the sample catalysts were investigated using an ASAP2020 Surface Area and Porosity Analyzer (Micromeritics, U.S.A.). Mössbauer spectra were obtained at the room temperature by MS 500 (Oxford Instruments, U.K.).

S1.4 Electrochemical measurements:

Electrochemical measurements were performed with a three-electrode configuration. The working electrodes were the commonly used thin-film rotating-disk-electrode (RDE) made by coating the catalyst samples as a thin film onto a glass carbon (GC) RDE substrate (diameter: 5 mm) with Nafion as the binding agent. To prepare the nonprecious metal electrodes, 10 mg catalysts were dispersed in 1 mL Nafion-isopropyl alcohol solution (2 mL 5 wt % Nafion mixed with 48 ml isopropyl alcohol) to form the catalyst inks and 12 μL ink suspension was pipetted onto the GC RDE. To prepare the Pt/C-loaded electrode, 5 mg catalyst was dispersed ultrasonically in 1 mL solution of Nafion in isopropyl alcohol (1 mL 5 wt % Nafion mixed with 49 ml isopropyl alcohol). 4 μL of the resulted suspension was then pipetted onto a glass carbon (GC) rotating disk electrode (RDE, geometric area: 0.196 cm^2) to form a thin catalyst film. The catalyst loadings were respectively 0.6 mg cm^{-2} for non-precious metal catalysts and 0.1 mg cm^{-2} for Pt/C (20 μg cm^{-2} for Pt).

Prior to use, GC electrode was polished with 0.05 μm gamma Alumina powders, then rinsed thoroughly with ethanol and water in an ultrasonic bath to remove any alumina residues, and finally dried in the infrared lamp. The counter electrode was a Pt foil. The reference electrode used in 0.1 M $HClO_4$ aqueous solution was a saturated calomel electrode (SCE), which were separated from the working electrode by a Luggin capillary. However, all the potentials were expressed on the scale of the reversible hydrogen electrode (RHE) in this paper. To calibrate the SCE to the RHE scale, the steady-state polarization curves for hydrogen electrode reactions (HERs) were recorded at a potential scanning rate of 5 mV s^{-1} in a standard three-electrode system with Pt/C-loaded GC as the working electrode and Pt foil as the counter electrode, and the potentials at which the current crossed zero was taken as the RHE zero potential.

Before each measurement, the solutions were first purged with the high-purity Ar (for CVs), O_2 (for ORR polarization curves) for about 30 minutes, or H_2 (for HER polarization curves) for about 1 hour. The gases were allowed to flow above the solution during the measurements. The working electrode was first subject to potential cycling of 0.0 ~ 1.3 V before recording the CVs and the polarization curves for HERs and ORR under a potential scan rate of 500 mV s^{-1}. Such an electrochemical polish could get rid of the surface contaminations of the catalyst materials that could complicate the electrochemical measurements. Usually, the voltammetric responses in the first a few cycles changed significantly. After about 10 ~ 20 cycles, the successive cycling would give relatively steady voltammetric responses.

S2. XRD patterns for GO and the precursor mixture for the composite

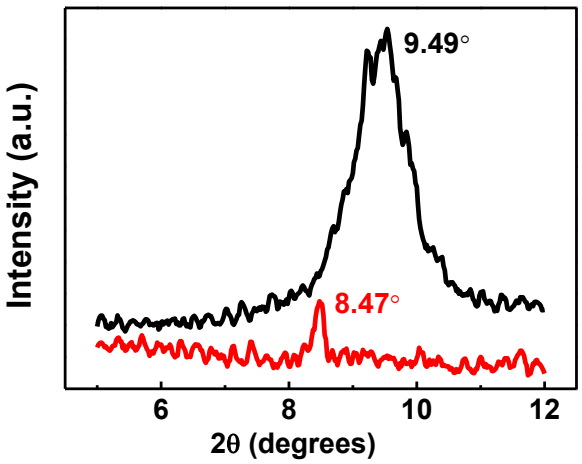

Figure. S1 XRD patterns of GO (black) and the precursor mixture containing GO, melamine and Fe salt (red).

S3. XPS results and analysis

The N1s spectra of the N-doped materials can be deconvolved into four peaks centered at 398.3 eV, 400.2 eV, 401.4 eV and 403.1 eV, which correspond to pyridinic-N, pyrrolic-N, graphitic-N and N-“O” (oxidized nitrogen) respectively. The Fe 2p spectra indicated the existence of the elementary and oxidized states of Fe in the composite.

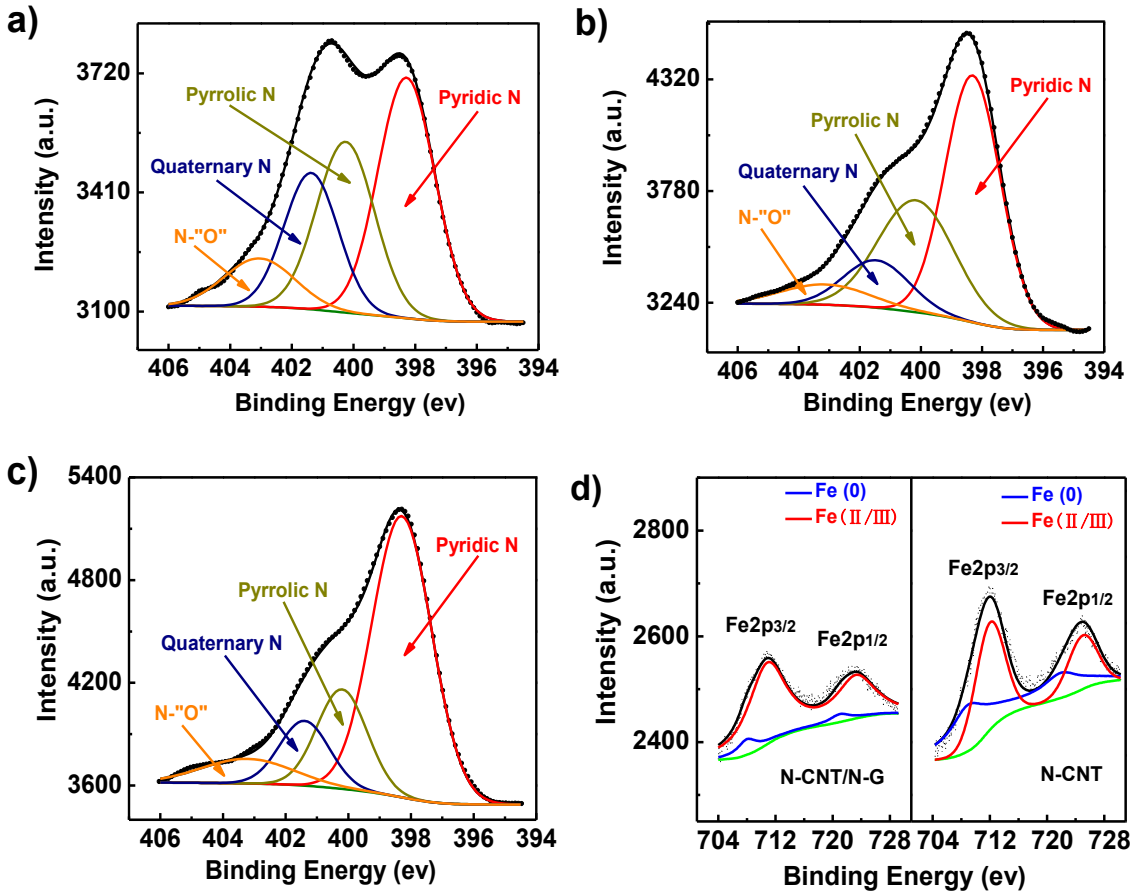

Figure. S2 XPS spectra of N1s narrow-scan and the corresponding deconvolution into components of different N functionalities for a) the N-CNT, b) the N-G and c) the N-CNT/N-G composite, and d) spectra of Fe 2p narrow-scan for the N-CNT/N-G composite. The black dotted lines are the measured spectra. The black solid lines are the superposition of the deconvolved spectra.

Table S1. N and Fe Speciation (at %) from XPS analysis for different materials

	N (at %)				Fe (at %)	
	Pyridinic N	Pyrrolic N	Quaternary N	“N-O”	Fe(0)	Fe(2+/3+)
N-CNT/N-G	4.01	1.19	0.78	0.53	0.04	0.76
N-CNT	1.79	1.29	0.96	0.44	0.66	0.78
N-G	3.05	1.9	0.7	0.4	/	/

S4. Mössbauer results and analysis

Mössbauer spectra were obtained at the room temperature by Oxford Instruments MS 500 with a standard ^{57}Co (Rh) Mössbauer source. Velocity scale and isomer shift δ_{iso} were calibrated against natural iron (α-Fe-foil, 25 μm thick, 99.99% purity). The δ_{iso} from calibration was used to be the gravity center for the fitting procedure. The spectroscopic data were analyzed by using the program "Recoil" with fitting parameters unfixed. The Mössbauer spectra of both catalysts were fitted with singlet, doublet, and sextet lines. (see Table S2).

Table S2. Mössbauer parameters for the fitted lines and their assignments

Sample		δ_{iso} (mm/)	E_Q (mm/)	H_0 (T)	Real area **A** (%)	Assignment	Refs.
N-CNT/N-G	Singlet	0.23	0	0	18.4	FeN /γ-Fe	2,3
	Doublet1	0.57	1.41	0	18.0	C-Fe-N_2	4,5
	Doublet2	0.20	2.92	0	41.0	Fe-N_4 (distorted/MS)	4,5
	Sextet1	-0.01	0.92	30.0	2.0	α-Fe	3
	Sextet2	0.35	-0.48	13.4	20.6	$Fe_2C_xN_{1-x}$/ Fe_xN	2,6
N-CNT	Singlet	-0.08	0	0	23.2	FeN /γ-Fe	2,3
	Doublet1	0.39	0.94	0	1.8	Fe-N_4 (in-plane/LS)	4,5
	Doublet2	1.05	1.71	0	8.3	C-Fe-N_2	4,5
	Sextet1	0.002	0.01	32.4	46.2	α-Fe	3
	Sextet2	0.36	-0.28	24.2	5.7	$Fe_2C_xN_{1-x}$/ Fe_xN	2,6,7
	Sextet3	0.24	0.1	20.2	14.8	Fe_5C_2	8,9

Singlet:

The singlet found in the N-CNT/N-G composite (δ_{iso} = 0.16 mm s^{-1}) and the N-CNT (δ_{iso} = -0.08 mm s^{-1}) may be assigned to a FeN phase (δ_{iso} = 0.09 mm s^{-1}) as observed by Yang. *et al*[2] in the carbon nanotubes encapsulating cubic FeN nanoparticles, or the paramagnetic or the superparamagnetic γ-Fe phase (δ_{iso} = -0.1 mm s^{-1}) as reported by Prudnikava. *et al*[3] for the carbon nanotubes prepared by the injection CVD method using ferrocene-xylene solution.

Doublets:

The doublet1 (δ_{iso} = 0.56 mm s^{-1}, E_Q = 1.44 mm s^{-1}) and the doublet 2 (δ_{iso} = 0.21 mm s^{-1}, E_Q = 2.64 mm s^{-1}) in the composite may be associated with the C-Fe-N_2 and FeN_4 species. Similar results were reported by Koslowski. *et al*[4] for catalysts with iron porphyrin structures. The authors attributed a doublet of 0.35 mm s^{-1} δ_{iso} and 1.45 mm s^{-1} E_Q to C-Fe-N_2 specie and a doublet of 0.3 mm s^{-1} δ_{iso} and 2.61 mm s^{-1} E_Q to distorted Fe-N_4 structure. In addition,

Kramm. *et al*[5] investigated catalysts prepared by heat-treatment of iron porphyrin impregnated on a carbon black and associated two doublets having (δ_{iso}, E_Q) of (0.4 mm s^{-1}, 1.66 mm s^{-1}) and (0.24 mm s^{-1}, 2.68 mm s^{-1}) with the C-Fe-N_2 and Fe-N_4 (ferrous mid-spin FeN_4) centers respectively.

The doublet1 (δ_{iso} = 0.39 mm s^{-1}, E_Q = 0.94 mm s^{-1}) in the N-CNT can be attributed to in-plane FeN_4 structures as that found by Koslowski. *et al*[4] (δ_{iso} = 0.33 mm s^{-1}, E_Q = 0.90 mm s^{-1}) for catalysts with iron porphyrin structures, and by Kramm. *et al*[5] (δ_{iso} = 0.30 mm s^{-1}, E_Q = 0.88 mm s^{-1}) for catalysts prepared by heat-treatment of iron porphyrin impregnated on a carbon black. The doublet 2 (δ_{iso} = 1.05 mm s^{-1}, E_Q = 1.71 mm s^{-1}) may be associated with C-Fe-N_2 according to its E_Q values.[4,5]

Sextets:

The sextet1 found in the N-CNT/N-G composite (δ_{iso} = -0.08 mm s^{-1}, E_Q = 0.56 mm s^{-1}, H_0 = 31.01 T) and the N-CNT (δ_{iso} = 0.002 mm s^{-1}, E_Q = 0.01 mm s^{-1}, H_0 = 32.4 T) should be due to the ferromagnetic α-Fe which exhibited magnetically split sextet.[3]

The sextet 2 in N-CNT/N-G composite could be due to Fe_xN as shown by Borsa. *et al*[6] (δ_{iso} = 0.28 mm s^{-1}, H_0 = 17.9 T) or $Fe_2C_xN_{1-x}$ phase observed by Yang. *et al*[2] (δ_{iso} = 0.23 mm s^{-1}, E_Q = 0.2 mm s^{-1}, H_0 = 15.9 T).

The sextet 2 in the N-CNT was similar to that found by Borsa. *et al*[6] (δ_{iso} = 0.28 mm s^{-1}, H_0 = 24.6 T) in various iron nitrides. Gajbhiye. *et al*[7] also obtained a sextet (δ_{iso} = 0.43 mm s^{-1}, E_Q = -0.85 mm s^{-1}, H_0 = 24.78 T) in nanostructured Fe nitrides. Thus, we can ascribe the sextet 2 in the N-CNT to Fe nitrides.

The sextet 3 found in N-CNT may be explained as the magnetic Fe_5C_2 phase as observed in the Mössbauer study of the $Fe_{1-x}C_x$ amorphous alloys at the room temperature by Bauer-Grosse. *et al*[8] (δ_{iso} = 0.22 mm s^{-1}, H_0 = 22.2 T). In addition, a very similar sextet (δ_{iso} = 0.24 mm s^{-1}, E_Q = -0.07 mm s^{-1}, H_0 = 20.2 T) was obtained by Tao. *et al*[9] in investigating a precipitated iron-based Fischer-Tropsch synthesis catalyst with Mössbauer spectroscopy, which was attributed to Fe_5C_2 phase.

S5. Koutecky-Levich analysis

Electron transfer numbers (n) were calculated using Koutecky-Levich equation:[10]

$$i^{-1}=i_k^{-1}+i_l^{-1}=i_k^{-1}+1/(0.62nFAD_{O2}^{2/3}\omega^{1/2}\upsilon^{-1/6}C_0) \quad \text{(eq S1)}$$

Where, i is the catalyst current measured; i_k is the kinetic current; i_l is the diffusion-limited current; n is the number of electrons exchanged per mole of O_2; F is the Faraday constant (96500 C mol^{-1}); A is electrode area (0.196 cm^{-2}); D_{O2} is the diffusion coefficient of O_2 in 0.1 M $HClO_4$ solution (2.0×10^{-5} cm^2 s^{-1}); ω is the rotation rate (rad s^{-1}); υ is the kinetic viscosity of the water (0.01 cm^2 s^{-1}) and C_0 is bulk concentration of O_2 in 0.1 M $HClO_4$ solution (1.2×10^{-6} mol cm^{-3}). The slope of the plot of reciprocal current (i^{-1}) versus the reciprocal square root of rotation rate ($\omega^{-1/2}$) gives n values by using the known parameters mentioned above.

S6. RRDE analysis

The rotating ring-disk electrode (RRDE) measurements for the N-CNT/N-G catalyst were also performed with a three-electrode system in O_2-saturated 0.1 M KOH solution at a rotation rate of 1600 rpm. The H_2O_2 percentage released during ORR and the apparent electrons transferred numbers were calculated based on the following equations:[11]

$$n=4I_D/[I_D+(I_R/N)] \quad \text{(eq S2)}$$

$$\%H_2O_2 = 200I_R / (N*I_D+I_R) \quad \text{(eq S3)}$$

Where I_D and I_R represent the disk and ring currents respectively, and N is the current collection efficiency of the Pt ring, which was 0.25 in our system.

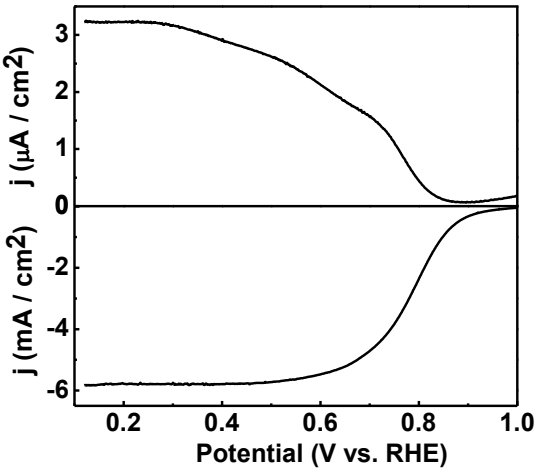

Figure. S3 RRDE test of the ORR for N-CNT/N-G.

S7. Stability of the N-CNT/N-G composite catalyst under potential cycling

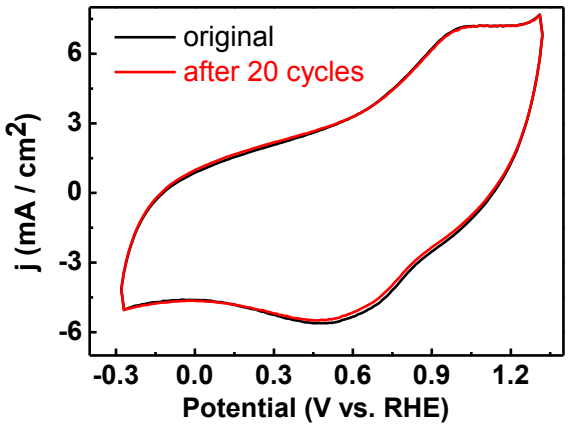

Figure. S4 Cyclic voltammograms of the N-CNT/N-G catalyst before and after 20 cycles of potential cycling in 0.1 M $HClO_4$.

S8. Effect of Fe content in the precursor mixture and heating temperature on the ORR activities of the composites

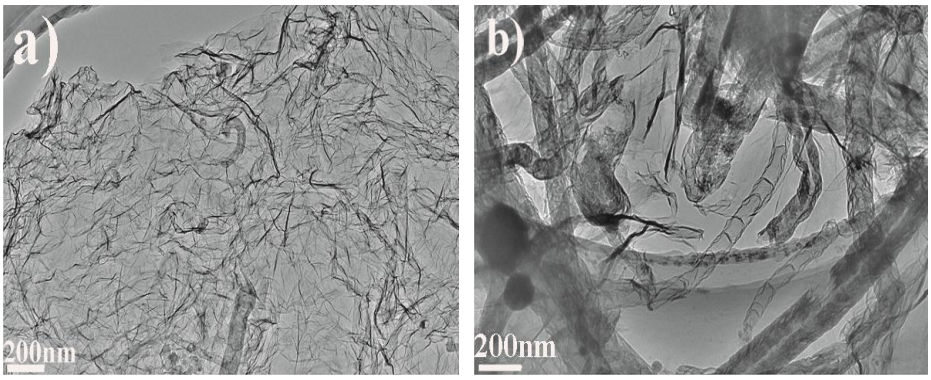

Figure. S5 TEM images of the N-CNT/N-G composites prepared from precursor mixtures with Fe/GO mass ratios of a) 1:75 and b) 1:15 respectively.

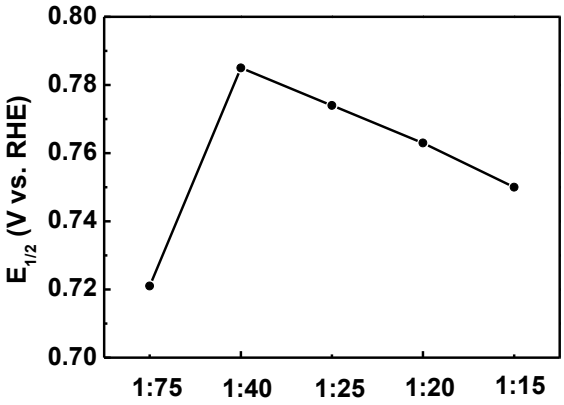

Figure. S6 Variation of the half wave potential ($E_{1/2}$) in the ORR polarization curves for the N-CNT/N-G composites prepared from precursor mixtures with different Fe/GO mass ratios.

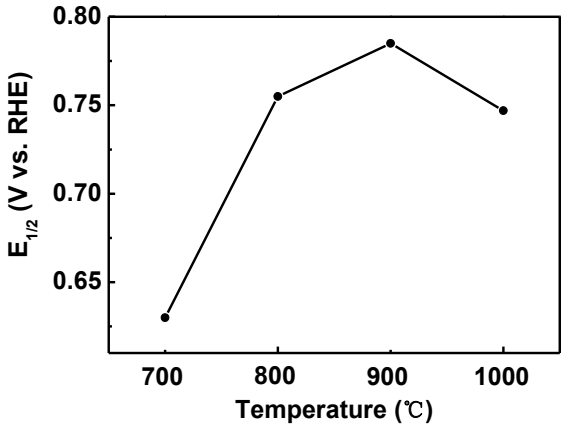

Fig. S7 Variation of the half wave potential ($E_{1/2}$) in the ORR polarization curves for the N-CNT/N-G composites prepared at different temperatures.

References

1 S. Yoshimoto, J. Inukai, A. Tada, T. Abe, T. Morimoto, A. Osuka, H. Furuta and K. Itaya, *J. Phys. Chem. B*, 2004, **108**, 1948.

2 Z. Yang, S. Guo, X. Pan, J. Wang and X. Bao, *Energy Environ. Sci*., 2011, **4**, 4500.

3 A. L. Prudnikava, J. A. Fedotova, J. V. Kasiuk, B. G. Shulitski and V. A. Labunov, *Semiconductor Physics, Quantum Electronics & Optoelectronics*., 2010, **13**, 125.

4 U. I. Koslowski, I. Abs-Wurmbach, S. Fiechter and P. Bogdanoff, *J. Phys. Chem. C*, 2008, **112**, 15356.

5 U. I. Kramm, I. Abs-Wurmbach, I. Herrmann-Geppert, J. Radnik, S. Fiechter and P. Bogdanoff, *J. Electrochem. Soc*., 2011, **158**, 69.

6 D. M. Borsa and D. O. Boerma, *Hyperfine Interact.*, 2003, *151/152*, 31.

7 N. S. Gajbhiye, R. N. Panda, R. S. Ningthoujam and S. Bhattacharyya, *phys. stat. Sol.*, 2004, **12**, 3252.

8 E. Bauer-Grosse, G. Le Caër and L. Fournes, *Hyperfine Interactions.* 1986, **27**, 297.

9 Z. Tao, Y. Yong, C. Zhang, T. Li, M. Ding, H. Xiang and Y. Li, *J. Natural Gas Chem.*, 2007, **16**, 278.

10 D. Yang, A. Velamakanni, G. Bozoklu, S. Park, M. Stoller, R. Piner, S. Stankovich, I. Jung, D. Field, C. Ventrice Jr and R. Ruoff, *Carbon*, 2009, **47**, 145.

11 Z.-S. Wu, S. Yang, Y. Sun, K. Parvez, X. Feng and K. Müllen, *J. Am. Chem. Soc.*, 2012, **134**, 9082.